JOURNAL OF VIROLOGY, Aug. 2010, p. 7459–7472 Vol. 84, No. 15
0022-538X/10/$12.00 doi:10.1128/JVI.01875-09

Processing of Lagging-Strand Intermediates *In Vitro* by Herpes Simplex Virus Type 1 DNA Polymerase▽

Yali Zhu,[1] Zetang Wu,[2] M. Cristina Cardoso,[3] and Deborah S. Parris[1,2]*

Department of Molecular Virology, Immunology, and Medical Genetics,[1] and Program in Molecular, Cellular, and Developmental Biology,[2] Ohio State University, Columbus, Ohio 43210; and Department of Biology, Technische Universität Darmstadt, Schnittspahnstrasse 10, D-64287 Darmstadt, Germany[3]

Received 3 September 2009/Accepted 28 April 2010

The processing of lagging-strand intermediates has not been demonstrated *in vitro* for herpes simplex virus type 1 (HSV-1). Human flap endonuclease-1 (Fen-1) was examined for its ability to produce ligatable products with model lagging-strand intermediates in the presence of the wild-type or exonuclease-deficient (exo$^-$) HSV-1 DNA polymerase (pol). Primer/templates were composed of a minicircle single-stranded DNA template annealed to primers that contained 5′ DNA flaps or 5′ annealed DNA or RNA sequences. Gapped DNA primer/templates were extended but not significantly strand displaced by the wild-type HSV-1 pol, although significant strand displacement was observed with exo$^-$ HSV-1 pol. Nevertheless, the incubation of primer/templates containing 5′ flaps with either wild-type or exo$^-$ HSV-1 pol and Fen-1 led to the efficient production of nicks that could be sealed with DNA ligase I. Both polymerases stimulated the nick translation activity of Fen-1 on DNA- or RNA-containing primer/templates, indicating that the activities were coordinated. Further evidence for Fen-1 involvement in HSV-1 DNA synthesis is suggested by the ability of a transiently expressed green fluorescent protein fusion with Fen-1 to accumulate in viral DNA replication compartments in infected cells and by the ability of endogenous Fen-1 to coimmunoprecipitate with an essential viral DNA replication protein in HSV-1-infected cells.

Herpes simplex virus type 1 (HSV-1), the prototypic member of the family of *Herpesviridae* and that of the alphaherpesviridae subfamily, has served as the model for understanding the replication of herpesvirus genomes during lytic virus replication (29). The 152-kbp genome of herpes simplex virus type 1 (HSV-1) possesses approximately 85 genes, 7 of which have been shown to be necessary and sufficient for viral DNA replication within host cells (reviewed in references 5 and 38). These seven genes encode a DNA polymerase (pol) and its processivity factor (UL42), a heterotrimeric complex containing a DNA helicase (UL5), primase (UL52), and noncatalytic accessory protein (UL8), a single-stranded DNA binding protein (infected cell protein 8 [ICP-8]), and an origin binding protein with DNA helicase activity (UL9). There is strong evidence in support of the circularization of the linear virion DNA shortly after entry, and DNA replication then is thought to initiate at one or more of the three redundant origins of replication (29, 38). At least in the earliest stages of viral DNA replication, UL9 protein is required, presumably to bind to and unwind the DNA and to attract the other DNA replication proteins (29, 38). The electron microscopic examination of pulse-labeled replicating HSV-1 DNA indicates the presence of lariats, eye-forms, and D-forms (21), which is consistent with bidirectional theta-like replication from origins. To date, however, no biochemical assay has demonstrated origin-dependent DNA replication *in vitro*. However, in the absence of UL9, the other six HSV DNA replication proteins can support initiation and replication from a circular single-stranded DNA (ssDNA) template in an origin-independent fashion (15, 26), resembling the rolling-circle mode of replication thought to occur during the later stages of viral replication.

Although nicks and small gaps have been observed in isolated replicating and virion DNA (38), the evidence for bidirectional duplex synthesis, the rapid rate of viral DNA replication, and the absence of long stretches of ssDNA in replicating and mature DNA isolated from HSV-1-infected cells suggest that leading- and lagging-strand synthesis are closely coordinated *in vivo*. Falkenberg et al. (15) used a minicircle DNA template with a strand bias and the six essential HSV-1 DNA replication proteins needed for rolling circle replication to demonstrate lagging-strand synthesis *in vitro*. However, replication from the parental strand template (leading-strand synthesis) was more efficient than synthesis from the complementary-strand template (lagging-strand synthesis). These results suggest the possibility that one or more host functions required for efficient lagging-strand synthesis or for its close coordination with leading-strand synthesis is missing in such *in vitro* systems.

Although leading- and lagging-strand syntheses share many of the same requirements for bulk DNA synthesis, lagging-strand synthesis is a more complex process. Because the direction of polymerization of lagging-strand intermediates is opposite the direction of replication fork movement, lagging-strand synthesis requires that priming and extension occur many times to produce discontinuous segments called Okazaki fragments (reviewed in reference 25). Okazaki fragments need to be processed to remove the RNA primer, to fill in the area previously occupied by the RNA, and to seal the remaining nick between fragments, all of which must occur efficiently, accurately, and completely. Failure to do so would result in the

* Corresponding author. Mailing address: Department of Molecular Virology, Immunology, and Medical Genetics, Ohio State University, 2198 Graves Hall, 333 West Tenth Ave., Columbus, OH 43210. Phone: (614) 292-0735. Fax: (614) 292-9805. E-mail: parris.1@osu.edu.

▽ Published ahead of print on 5 May 2010.

accumulation of DNA breaks, multiple mutations, delayed DNA replication, and/or cell death (16, 61).

In eukaryotes, what is currently known regarding the process of lagging-strand synthesis is based on genetic and biochemical studies with *Saccharomyces cerevisiae* and on *in vitro* reconstitution studies to define the mammalian enzymes required for simian virus 40 (SV40) T-antigen-dependent DNA replication (17, 37, 44, 57, 58). These studies have revealed that the extension of a newly synthesized Okazaki fragment DNA with pol δ causes the strand displacement of the preceding fragment to produce a 5′ flap (25). Results suggest that flap endonuclease 1 (Fen-1) is the activity responsible for the removal of the bulk of the 5′ flaps generated (1, 44, 48), although dna2 protein may facilitate the removal of longer flaps coated with the ssDNA binding protein complex (2, 44). In addition, the overexpression of exonuclease I can partially compensate for the loss of Fen-1 function in yeast (24, 51). For the proper processing of lagging-strand intermediates, the entire 5′ flap and all of the RNA primer need to be removed, and the gap must be filled to achieve a ligatable nick. DNA ligase I has been shown to be the enzyme involved in sealing Okazaki fragments in yeast and in humans (3, 31, 50, 56, 57). DNA ligase I requires a nick in which there is a 5′ phosphate on one end and a 3′ hydroxyl linked to a deoxyribose sugar entity on the other, and it works poorly in the presence of mismatches (54). The close coordination of Fen-1 and DNA ligase I activities for Okazaki fragment processing is facilitated by the interactions of these proteins with proliferating cell nuclear antigen (PCNA), the processivity factor for pol δ and ε (6, 30, 32, 46, 52, 53).

HSV-1 does not appear to encode a protein with DNA ligase activity or one that can specifically cleave 5′ flaps, although it does encode a 5′-to-3′ exonuclease activity (UL12 [10, 20]) and a 3′-to-5′ exonuclease activity that is part of the HSV-1 pol catalytic subunit (27). As for most eukaryotes, RNA primers are essential for HSV-1 DNA synthesis, as demonstrated by the presence of oligoribonucleotides in replicating DNA *in vivo* (4), by the well-characterized ability of the UL52 protein in complex with the UL5 helicase activity to synthesize oligoribonucleotide primers on ssDNA *in vitro* (11, 13), and by the requirement of the conserved catalytic residues in the UL52 primase *in vitro* and in HSV-1-infected cells (14, 26). It is the strand displacement activity of pol δ that produces the 5′ flaps that are key to the removal of RNA primers during Okazaki fragment processing (6, 25). However, we previously demonstrated that wild-type HSV-1 DNA polymerase possesses poor strand displacement activity (62), in contrast to mammalian DNA pol δ (25). Thus, it is not apparent how RNA primers would be removed when encountered by HSV-1 pol during HSV-1 lagging-strand synthesis or how such intermediates would be processed.

We wished to test the hypothesis that the nick translation activity of mammalian Fen-1 could function in collaboration with HSV-1 pol to facilitate the proper removal of RNA primers and/or short flaps to produce the ligatable products required for Okazaki fragment processing. In this report, we have examined the ability of wild-type and exonuclease-deficient (exo$^-$) HSV-1 pol, which differ in their respective strand displacement activities, to extend model lagging-strand substrates in the presence or absence of mammalian Fen-1. Our results demonstrate that both wild-type and exo$^-$ HSV-1 pol can cooperate with and enhance Fen-1 activity to achieve a ligatable nick *in vitro*. Moreover, colocalization and coimmunoprecipitation studies reveal a physical association of Fen-1 with HSV-1 DNA replication proteins, supporting a model for the involvement of Fen-1 in HSV-1 DNA replication.

MATERIALS AND METHODS

Preparation of enzymes. The HSV-1 genes encoding the wild-type or exo$^-$ (D368A) DNA polymerase catalytic subunits (pol) were expressed in Sf9 insect cells from the polyhedrin promoter of recombinant baculoviruses. The wild-type and exo$^-$ pol recombinants were the gifts of Robert Lehman (Stanford University) and Charles Knopf (University of Heidelberg), respectively, and were purified as detailed previously (8, 45). A plasmid construct encoding human DNA ligase I tagged with eight histidine residues at the N terminus (pHIS-hLIG1) was the kind gift of Robert Bambara (University of Rochester). Purified his-tagged DNA ligase I was obtained from transformed *Escherichia coli* 6 h following induction by isopropyl-β-D-1-thiogalactopyranoside (IPTG) as described previously, and the function of this enzyme has been shown to be indistinguishable from that of the enzyme without the tag (19). The purity of the DNA ligase and HSV-1 polymerases was deemed to be >95% as assessed by silver-stained gels following denaturing polyacrylamide electrophoresis. Purified human Fen-1 was purchased from Trevigen, Inc. (Gaithersburg, MD).

Preparation of DNA substrates. Fig. 1 shows the DNA sequence and primer/templates (P/Ts) utilized. The lower strand (Fig. 1A) was circularized as previously described by annealing it to a 20-nucleotide (nt) bridge fragment complementary to both ends, followed by ligation with T4 DNA ligase to form a 70-nt minicircle (62). The gel-purified minicircle served as the template for all forms of P/T. All upper strands (unphosphorylated) were synthesized and gel purified by the manufacturer (IDT, Coralville, IA). The complementary primer strands for the B (50/70) and D P/Ts were identical, except that D also contained a 5′ flap structure composed of a 20-nt oligo(dT) sequence (dT_{20}50/70). The P/T shown in Fig. 1C was a nicked open minicircle (70/70) that contained all of the B form primer sequences as well as an additional 20 nt of sequences complementary to the gap. Form E P/T (R_{10}40/70) contained primer sequences identical to those of form B, except that the first 10 residues at the 5′ end were ribonucleotides. All primers were labeled at the 5′ end using [γ-^{32}P]ATP and T4 polynucleotide kinase according to standard procedures. The respective primers were mixed with the 70-nt minicircle at a 1:1 molar ratio, heated to 55°C for 10 min, and slowly cooled to room temperature to produce the DNA P/Ts.

Enzyme assays. The presence of the various enzymes is indicated for each experiment. A final concentration of 50 nM was used for each of the polymerases. The concentration of Fen-1 selected (0.01 U/μl) was that required to cleave 80% of flaps from 0.5 nM dT_{20}50/70 DNA P/T (Fig. 1D) in 20 min at 30°C. The concentration of DNA ligase I selected (30 nM) was that which permitted the ligation of approximately 60% of the 70/70 DNA P/T (Fig. 1C) in 20 min at 30°C. In some experiments, as indicated, Fen-1 was heat inactivated by incubation for 10 min at 75°C. Enzymes were incubated as indicated with DNA P/Ts (0.5 nM) for 10 min at 30°C in buffer containing 60 mM Tris-Cl, pH 8.0, 25 mM NaCl, 5 mM dithiothreitol, 0.1 mg/ml bovine serum albumin (BSA), 10% glycerol, 3 mM ATP, 250 μM (each) dATP, dCTP, dGTP, and dTTP (Amersham Biosciences, Piscataway, NJ), and 2.5 mM EDTA. In some cases, as indicated, [α-^{32}P]dATP (MP Biomedicals, Irvine, CA) was included to facilitate the tracking of all products. Reactions were initiated by the addition of $MgCl_2$ to a final concentration of 6 mM, portions were removed at various times, and the reactions were terminated by the addition of EDTA to a final concentration of 50 mM. Products were separated by electrophoresis through denaturing gels containing 10% polyacrylamide and 6 M urea, unless otherwise indicated. For the analysis of nick translation reactions, products were separated by electrophoresis through long sequencing-style denaturing gels containing 20% polyacrylamide and 7 M urea. Size markers for nick translation experiments were generated by the digestion of the 50-nt ssDNA primer with the 3′-to-5′ exo activity of the HSV-1 wild-type pol for various times at 37°C. All gels were analyzed by exposure to a storage phosphor screen (Molecular Dynamics, Inc., Sunnyvale, CA) followed by scanning with a Typhoon 9200 variable-mode imager (GE Healthsciences, Piscataway, NJ). Products formed in the presence of unlabeled nucleotides were quantified using ImageQuant software as previously described (9, 45).

Immunoprecipitation and immunodetection. Immunoprecipitations were conducted using mouse monoclonal antibody to Fen-1 (SC-71101; Santa Cruz, Inc.), HSV-1 UL42 protein (Z1F11; gift of Howard Marsden; University of Glasgow

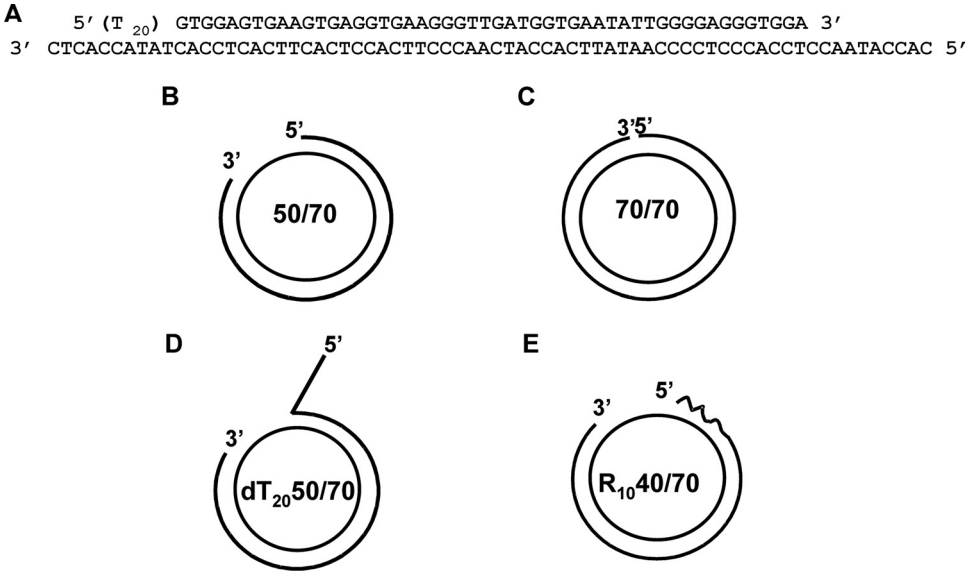

FIG. 1. Model primer/templates. All templates employ an ssDNA circular molecule 70 nt in length annealed to a variety of primers. (A) The sequences common to all primer/templates (P/Ts) as well as the 20-nt oligo(dT) flap (T_{20}) used for some of the P/Ts are shown. The bottom strand represents the circular DNA template that was prepared as described in Materials and Methods. The top strand represents the complementary 50-nt sequence in all primers and the 5′ T_{20} flap used for some. (B) The 50-nt DNA primer is annealed to the circular template to create a 20-nt gap. (C) The annealed DNA primer contains an additional 20 nt complementary to the circular template to create an open circular molecule with a ligatable nick. (D) The primer strand contains oligo(dT) residues at the 5′ end of the 50-nt complementary sequence to form a 5′ flap and a 20-nt gap at the 3′ end. (E) The 50-nt complementary primer is composed of 10 RNA residues at the 5′ end (wavy line) linked to 40 residues of DNA and annealed to the 70-nt circular template.

[41]), or isotype control (anti-myc antibody R950-25; Invitrogen, Carlsbad, CA). Antibodies were bound to Protein G-agarose (Sigma, St. Louis, MO) by incubation overnight at 4°C using a ratio of 2 μg Fen-1 or myc antibody or 10 μl UL42 antibody to 25 μl protein G in 200 μl immunoprecipitation (IP) buffer (50 mM Tris-Cl, pH 8.0, 150 mM NaCl, 1% NP-40, 0.1% SDS, 1× Complete EDTA-free, and 1× Phostop [Roche Diagnostics, Indianapolis, IN]) containing 5% heat-inactivated BSA. Vero cells that were mock infected or infected with HSV-1 strain KOS at an input multiplicity of 10 PFU/cell were harvested at 8 h postinfection, flash frozen in liquid nitrogen, and stored at −80°C. Total cell extracts (~4×10^7 to 5×10^7 cells/ml) were prepared in IP buffer and clarified prior to incubation. Two hundred microliters of cell extract was incubated with 25 μl antibody-bound and washed protein G agarose for 2 h at 4°C. Agarose beads were pelleted by low-speed centrifugation, and supernatants were collected and stored at −80°C. Beads were washed at least four times in 200 volumes of IP buffer. Bound proteins were eluted in a total volume of 50 μl of dissociation buffer (65 mM Tris-Cl, pH 6.8, 1% SDS, 2.5% 2-mercaptoethanol, 10% glycerol, 0.002% bromophenol blue, final concentration), boiled for 10 min, and centrifuged at high speed, and the eluates were analyzed by SDS-PAGE. Proteins were transferred from gels to nitrocellulose membranes and immunoblotted using polyclonal rabbit antibody to Fen-1 (NB100-300; Novus Biologicals, LLC, Littleton, CO) diluted 1:5,000, monospecifc polyclonal rabbit antibody 834 to UL42 (40) diluted 1:500, or polyclonal rabbit antibody to human PCNA (A300-276A; Bethyl Laboratories, Inc., Montgomery, TX) diluted 1:2,000. Details of the preparation of the UL42 antibody 834 have been described already (40). Reactive bands were detected by incubation with a 1:10,000 dilution of horseradish peroxidase-conjugated goat anti-rabbit IgG using the SuperSignal West Pico chemiluminescence kit (Thermo Scientific, Rockford, IL). Membranes were exposed to X-ray film. In some cases, membranes subsequently were stripped twice for 20 min each at room temperature in buffer containing 1.5% glycine, 0.1% SDS, 1% Tween-20, pH 2.2, and reprobed with a different antibody.

Localization of proteins in cultured cells. The plasmid construct for the expression of green fluorescent protein (GFP) fused to the mouse Fen-1 gene has been described previously (46) and was expressed transiently in baby hamster kidney (BHK) cells. Briefly, BHK cells in 35-mm dishes were transfected with 600 ng of the plasmid using Lipofectamine 2000 transfection reagent (Invitrogen) according to the instructions of the manufacturer. After 42 to 48 h of incubation at 34°C, cells were washed three times with phosphate-buffered saline, fixed with 3.7% formaldehyde, and permeabilized with 0.25% Triton X-100. In some cases, areas of active DNA replication were identified by the incorporation of 5′ bromo-2-deoxyuridine (BrdU). The BrdU was added directly to the culture medium 30 min prior to fixation to achieve a final concentration of 100 μM. Areas of BrdU incorporation were detected by indirect immunofluorescence with mouse monoclonal antibody to BrdU (Becton-Dickinson, San Jose, CA) as the primary antibody and goat anti-mouse IgG labeled with either rhodamine isothiocyanate (RITC) or fluorescein isothiocyanate (FITC), as indicated for each experiment, as the secondary antibody. Viral DNA replication compartments in nontransfected or transfected cells were detected by the immunolocalization of the UL42 pol processivity factor essentially as described previously (18), except that cells were permeabilized with 0.25% Triton X-100 following formaldehyde fixation. Briefly, BHK cells were mock infected or infected with HSV-1 wild-type strain KOS (5 PFU/cell) 24 h after seeding (nontransfected) or 42 h following transfection and fixed 3 h postinfection. Indirect immunofluorescence was performed with monospecific rabbit antibody 834 directed to the immunodominant epitope of the UL42 protein, followed by incubation with RITC-conjugated goat anti-rabbit IgG. Confocal images were acquired with a laser-scanning microscope (LSM 510 META; Zeiss) using a 63× objective. GFP/FITC and RITC were excited at 488 and 543 nm, respectively. A multitrack mode was used to collect images sequentially. To ensure that there was no overlap in emission between channels, the green or red lasers were turned off sequentially prior to final image collection. In some cases, Z-stacks were collected throughout the depth of cells for three-dimensional reconstructions. The degree of the colocalization of proteins also was assessed by quantifying the intensities of signal from each channel along random lines drawn across the nuclei of cells in which the expression of both proteins was detected at nonsaturating levels.

Digital images. The contrast and brightness of digital images were adjusted using a linear relationship between signal and image intensity. Adjustments were identical across all lanes for each figure or figure panel to allow for the adequate visualization of low-intensity bands. However, the quantification of band intensity was always from unaltered storage phosphor data.

RESULTS

Gap filling by HSV-1 pol produces ligatable products. A salient feature of lagging-strand synthesis is the encounter of polymerase extending a new Okazaki fragment with the 5′ end

of the previously synthesized fragment. A well-studied eukaryotic polymerase involved in lagging-strand synthesis, *S. cerevisiae* pol δ, possesses strand displacement activity that facilitates the removal of RNA primers from lagging-strand intermediates by creating 5′-flapped structures that subsequently are cleaved by Fen-1 (1, 44). To model this process *in vitro*, we utilized a synthetic DNA P/T consisting of a 70-nt circular template annealed to a series of oligonucleotides to create a 20-nt gap (Fig. 1). We demonstrated previously that the HSV-1 wild-type pol catalytic subunit and the processive pol/UL42 heterodimer could efficiently extend the 3′ end of the primer of the 50/70 P/T (Fig. 1B) across the gap, but it possessed only a limited ability to displace the annealed 5′ end of the primer strand (62). We were interested in determining how the HSV-1 pol could process lagging-strand intermediates in the absence of substantial strand displacement activity. To begin to address this, it was important to more precisely measure the strand displacement capability of the HSV-1 pol. Because eukaryotic DNA ligase I in an ATP-dependent reaction can catalyze the formation of a phosphodiester bond from nicked DNA substrates but not from those containing gaps or flaps (39, 54), the production of ligatable products would be an extremely sensitive means to quantify the strand displacement activity of HSV-1 pol. Moreover, the completion of lagging-strand synthesis requires that the final product be ligatable. To determine the extent to which the gap-filling activity HSV-1 pol yielded a product that could be ligated, the 50/70-gapped DNA P/T (Fig. 1B) was incubated with HSV-1 pol in the presence or absence of human DNA ligase I. As expected, the ligase failed to form a phosphodiester bond with the gapped DNA P/T following incubation for up to 20 min (Fig. 2, lane 6), although efficient ligation (60% of the available P/T within 20 min) was observed with the control (Fig. 1C) 70/70 nicked P/T (Fig. 2, lane 2). Likewise, the incubation of the gapped P/T with pol alone yielded a 70-nt linear product but no ligated circles (Fig. 2, lanes 7 to 10). The reduced amount of P/T and product at extended times of incubation with pol alone likely reflects the degradation of the P/T by the 3′-to-5′ exo activity of pol when the deoxynucleoside triphosphate (dNTP) concentration becomes limiting due to the idling-turnover activity of pol (62). In the combined presence of HSV-1 pol and DNA ligase I, we observed increasing amounts of 70-nt circular DNA as a function of time (Fig. 2, compare lanes 11 to 14 to lane 2) such that 54% of the available P/T had been ligated by 20 min. These results confirm that HSV-1 pol fails to strand displace on the majority of P/Ts during gap-filling synthesis.

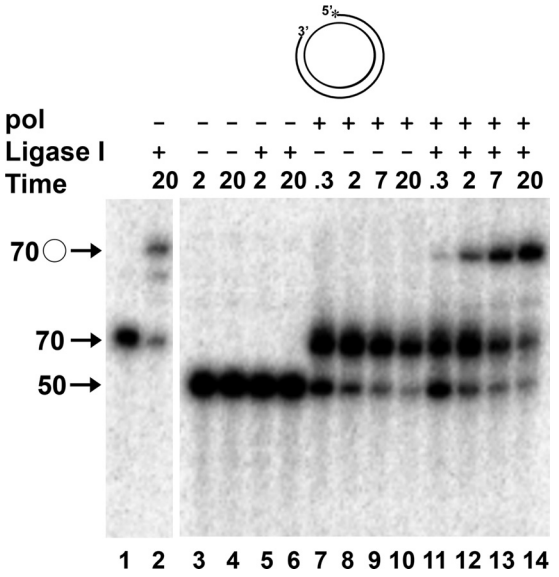

FIG. 2. Gap filling by HSV-1 pol creates ligatable nicks. Control ligation reactions were performed by incubating 0.5 nM 70/70 primer/template (Fig. 1C) without DNA ligase I (lane 1) or with DNA ligase I (lane 2) for 20 min. In lanes 3 to 14, reactions were performed with 0.5 nM 50/70 P/T (Fig. 1B) in which the primer strand was 5′ end labeled. The DNA was preincubated in the absence (−) or presence (+) of 50 nM HSV-1 pol catalytic subunit (pol) and/or 30 nM human DNA ligase I for 5 min at 30°C in the presence of EDTA. Reactions were initiated by the addition of $MgCl_2$ as described in Materials and Methods and were terminated at the times indicated with EDTA. Products were resolved by denaturing gel electrophoresis, and the amount of radioactivity in each was determined as a percentage of total radioactivity present as detailed in Materials and Methods. The migration positions of the 50-nt primer, the unligated 70-nt extended primer, and the 70-nt circular, ligated DNA (○) are shown.

Processing of model lagging-strand intermediates by HSV-1 pol and human Fen-1. Because Fen-1 has been shown to be a major player in the processing of the 5′ ends formed during the synthesis and processing of Okazaki fragments, we next examined the ability of human Fen-1 to cleave a 5′-flapped and gapped minicircle DNA P/T (dT_{20}50/70) (Fig. 1D) in the presence or absence of HSV-1 pol. Fen-1 and/or HSV-1 pol was incubated with the DNA P/T in the presence of EDTA for at least 5 min at 30°C. Control experiments demonstrated that there was no difference in DNA products with or without enzymes in the presence of EDTA (results not shown). The synchronous initiation of reactions was achieved by the addition of $MgCl_2$, and reactions were terminated with EDTA at various times up to 20 min. Extension and cleavage products were detected following boiling and electrophoresis through denaturing gels (Fig. 3).

In the absence of HSV-1 pol, Fen-1 cleaved 60% of the 5′ flap by 7 min (Fig. 3, lane 4). The analysis of products on a sequencing-style gel (not shown) revealed products of predominantly 21 nt with a minor population of 19-nt products, which is consistent with the specificity of Fen-1 cleavage previously reported (34). In the absence of Fen-1, HSV-1 pol extended 70% of the available DNA primers within the first 20 s, producing predominantly 90-nt products corresponding precisely to gap-filled molecules (Fig. 3, lane 8). In the presence of HSV-1 pol, Fen-1 cleaved the 5′ flap, and flap cleavage products increased as a function of time (Fig. 3, lanes 10 to 12). In contrast, no cleavage of flaps was observed following the incubation of P/T with heat-inactivated Fen-1 alone (Fig. 3, lanes 5 and 6) or with pol in the presence of heat-inactivated Fen-1 (Fig. 3, lanes 13 to 15). Moreover, the formation of 90-nt gap-filled products by HSV-1 pol was indistinguishable in the absence or presence of heat-inactivated Fen-1 (Fig. 3, compare lanes 7 to 9 with lanes 13 to 15). Thus, flap cleavage depends on Fen-1 enzymatic activity rather than the presence of the protein *per se*.

The ability of Fen-1 to cooperate with a mutant HSV-1 pol (D368A) also was assessed. This mutant pol possesses wild-type polymerizing ability but is completely deficient in the associated 3′-to-5′ exonuclease (exo) activity (28, 45). Unlike

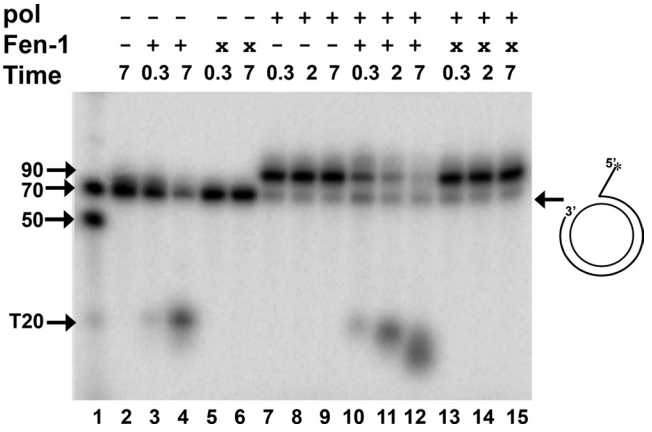

FIG. 3. Processing of model primer/templates by wild-type HSV-1 DNA polymerase and Fen-1 activities. The 5′-flapped model primer/template (dT_{20}50/70), depicted in Fig. 1D and at the right in this figure, contained a ^{32}P label at the 5′ end of the primer strand. All reaction mixes contained 0.5 nM annealed DNA, were preincubated in the presence of EDTA with the indicated enzymes for 5 min at 30°C, and were initiated by the addition of $MgCl_2$ as described in Materials and Methods. Reactions were terminated by the addition of EDTA at the times (in min) indicated, the reaction mixes were boiled, and the products were analyzed by denaturing electrophoresis. The presence or absence of the indicated enzymes is designated by a plus and minus sign, respectively. In some cases, head-inactivated enzyme was added (×). The final concentration of active enzyme, when present, was 50 nM for pol and 0.01 U/μl for Fen-1. Reaction mixtures containing no enzyme (lane 2) were incubated continuously in the presence of EDTA and define the zero time point for all reactions. The migration positions of marker oligonucleotides, including a 50- and 70-nt sequence complementary to the minicircle and a 20-nt oligo(dT) (T_{20}) (lane 1), are shown on the left. The migration position of the fully gap-filled product (90 nt) also is shown. The amount of radioactivity in each product was determined as a percentage of the total radioactivity present as detailed in Materials and Methods.

wild-type pol, exo$^-$ HSV-1 pol possesses substantial strand displacement activity (62). We reasoned that the close coordination of the strand displacement activity of the exo$^-$ pol and flap cleavage by Fen-1 would be manifest by the production of ligatable products. For these experiments, we used the 5′-flapped and gapped dT_{20}50/70 DNA P/T shown in Fig. 1D. The 5′ end of the primer was labeled with ^{32}P, and the reaction buffer also contained [α-^{32}P]dATP to allow the tracking of both Fen-1 cleavage and polymerase extension products. Thus, the intensity of label in the extended products was not directly proportional to the amount of DNA substrate used but varied as a function of the number of dA residues in extended products. The incubation of the dT_{20}50/70 DNA P/T with Fen-1 alone yielded products 21 nt or smaller in size (Fig. 4, lanes 17 and 18). As expected, the incubation of the DNA with human DNA ligase I in the absence of other enzymes failed to produce any ligated product (Fig. 4, lanes 15 and 16). In the absence of Fen-1 and DNA ligase I, 87% of the labeled P/T was extended by the wild-type or exo$^-$ D368A pol within 5 min (Fig. 4 lanes 1 and 19, compare to the no-enzyme controls in lanes 13 and 14). The more potent strand displacement activity of exo$^-$ pol is evident by sizes of products of >90 nt in length following a 20-min incubation (Fig. 4, lane 20). These larger products were confirmed by the analysis of products on long sequencing-style gels (not shown). However, when the wild-type HSV-1 pol was incubated together with Fen-1 and DNA ligase I, the amount of ligated circular 70-mer increased linearly as a function of time through 20 min (Fig. 4, lanes 9 to 11, compare to the no-enzyme controls in lanes 13 and 14). The decrease in the size of cleaved flaps was due to the 3′-to-5′ exo activity of the wild-type pol, because they were not observed in reaction mixtures containing the D368A exo$^-$ HSV-1 pol (Fig. 4, compare lanes 7 to 12 to lanes 21 and 22). Consistent with the strand displacement activity of the HSV-1 exo$^-$ pol, some flaps larger than 21 nt in size were observed in reactions that also contained Fen-1 (lanes 21 and 22). Despite the strand displacement activity of the mutant HSV-1 pol, ligated products were produced in the presence of exo$^-$ pol at more than twice the rate as that produced in the presence of wild-type pol during a 20-min period (Fig. 4, compare lanes 21 and 22 to lanes 9 to 11). Taken together, these results suggest that the Fen-1 cleavage of flaps, even in the presence of strand displacement activity, is closely coordinated with extension by HSV-1 pol to achieve a readily ligatable DNA product.

Extension by HSV-1 pol stimulates the nick translation activity of human Fen-1. The ability of Fen-1 to closely coordinate the cleavage of flaps with the gap-filling activity of HSV-1 pol, even in the presence of the strand displacement activity of exo$^-$ pol, did not explain how lagging-strand intermediates could be processed by wild-type pol, which failed to produce 5′ flaps on most P/Ts during gap-filling synthesis (Fig. 2). We hypothesized that the close coordination of Fen-1 and HSV-1 pol could be achieved by the stimulation of the nick translation activity of Fen-1 (i.e., the ability of Fen-1 to cleave short flaps generated by the displacement of 1 or 2 nt) by the HSV-1 pol. We examined the nick translation activity of Fen-1 in the presence of wild-type or exo$^-$ HSV-1 pol using the 5′-annealed 50/70 DNA P/T lacking a flap as shown in Fig. 1B. The annealed DNA was uniquely 5′ end labeled, and only unlabeled dNTPs were used for extension by the polymerases to permit the accurate quantification of cleavage products. To permit the high resolution of products, reactions were analyzed on sequencing-style gels together with DNA markers. At the times examined, most of the labeled reaction products were 3 nt or less (results not shown). Figure 5 shows the migration of products 1, 2, or 3 nucleotides in length. When incubated with the P/Ts alone, Fen-1 produced 1- and 3-nt products almost exclusively (Fig. 5A, lanes 8 to 11) compared to incubation in the absence of enzymes (lane 1). In contrast, when the P/T was incubated with Fen-1 and either wild-type or exo$^-$ pol, a rapid production of a 2-nt product was observed (Fig. 5A, lanes 14 to 17 and 24 to 27, respectively). During the 10-min reaction period, no labeled small (1 to 3 nt) products were observed following the incubation of the P/T with either wild-type pol or exo$^-$ pol alone. The formation of 1-, 2-, and 3-nt products by the various enzyme combinations was quantified and plotted as a function of time through 10 min (Fig. 5B, C, and D, respectively). The formation of each product through the first 2 min of the reaction is shown in the insets of each figure. From these plots, the initial rates of formation of each product was determined during the first 40 s of the reaction and are summarized in Table 1. The results demonstrate that the initial rate of formation of the primary product formed by the incubation of P/T with Fen-1 alone was enhanced approximately 2-fold with the additional presence of wild-type HSV-1 pol and 5-fold with

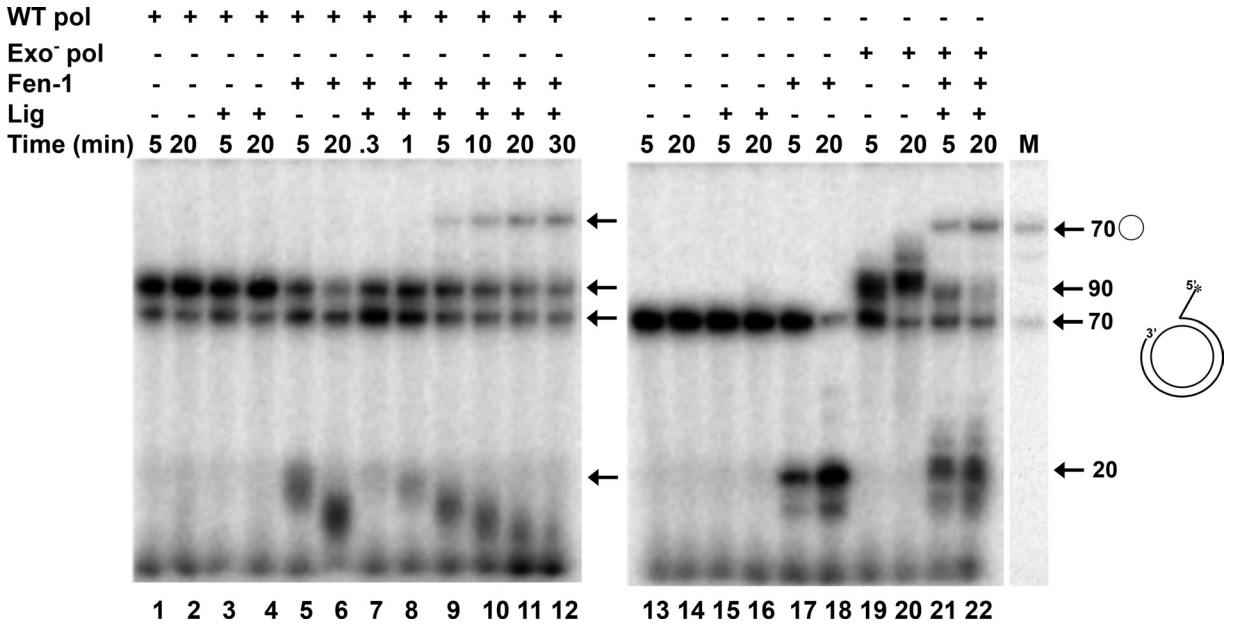

FIG. 4. Flap cleavage and DNA ligation with HSV-1 wild-type and exonuclease-deficient polymerase. The dT_{20}50/70 flapped primer/template (Fig. 1D and shown at the right in this figure) was used in all reactions, and the presence (+) or absence (−) of the wild-type HSV-1 pol catalytic subunit (WT pol; 50 nM), the exonuclease-deficient D368A pol catalytic subunit (Exo$^-$ pol; 50 nM), Fen-1 (0.01 U/μl), and/or DNA ligase I (Lig; 30 nM) in reaction mixtures is indicated above each lane. To track all products, the primer strand was 5′ end labeled with ^{32}P, and the dNTPs used for extension contained [α-^{32}P]dATP. Reactions were performed at 30°C and terminated with EDTA at the indicated times (in minutes) following initiation with $MgCl_2$. Products were resolved by denaturing electrophoresis through gels containing 12% polyacrylamide and 6 M urea. The migration positions of 20, 70, and 90 nt are shown, as is the circular product formed by the ligation of a control 70/70 P/T (lane M). Due to the presence of labeled dATP in reactions, the proportion of P/T extended was estimated from the radioactivity remaining at the 70-nt (linear) position compared to that present when no enzymes were added (lanes 13 and 14). The rate of the formation of ligated product was estimated by plotting the radioactivity in the bands corresponding to 70-nt circular product as a function of time and determining the slope of the linear portion by least-squares analysis.

the additional presence of exo$^-$ pol (Table 1). Likewise, the rate of formation of the minor 1-nt Fen-1 product was enhanced approximately 5-fold in the presence of wild-type pol and 10-fold in the presence of exo$^-$ pol. As expected, little or no 2-nt product was observed following the incubation of the 5′-annealed DNA P/T with only wild-type or exo$^-$ pol and appeared only after extended incubation with Fen-1 alone (Fig. 5 and Table 1). Nevertheless, the rate of formation of 2-nt product was enhanced at least 100-fold when both Fen-1 and either HSV-1 polymerase was present. The formation of this unique 2-nt product when both Fen-1 and polymerase are present, together with the enhanced rate of formation of Fen-1-specific 3- and 1-nt products, demonstrates that activities of the HSV-1 pol and Fen-1 are coordinated on DNA-containing P/Ts.

Because Okazaki fragments would be expected to contain annealed RNA at their 5′ ends and it is the primer RNA that must be removed to achieve a ligatable substrate, we utilized a P/T containing 10 nt of annealed RNA at the 5′ end (Fig. 1E) but that was otherwise identical to the 50/70-mer substrate shown in Fig. 1B. To distinguish it from the DNA P/T of the same size, we have called the RNA-containing substrate R_{10}40/70. To follow all of the products, the 5′ end of the primer was labeled with ^{32}P, and [α-^{32}P]dATP was included in reaction mixes (Fig. 6). Following the incubation of the R_{10}40/70 P/T in the presence of the wild-type HSV-1 pol alone, we observed only 70-nt extension products (Fig. 6, lanes 4 to 6). However, larger extension products were observed following incubation with the D368A exo$^-$ pol (Fig. 6, lanes 16 to 18), demonstrating the ability of this enzyme to displace annealed RNA. We confirmed that human DNA ligase I was unable to form a phosphodiester bond when the 5′ end contains a ribose sugar moiety on substrates gap filled by either the wild-type or exo$^-$ HSV-1 pol (lanes 10 to 12 and 22 to 24). However, in reactions that contained the wild-type or exo$^-$ HSV-1 pol, Fen-1, and DNA ligase I, ligated products were observed, particularly after longer times of incubation (Fig. 6, lanes 13 to 15 and 25 to 27, compared to the no-enzyme control in lane 1). Because extension alone by HSV-1 wild-type pol is not capable of producing a ligatable product and because incubation with pol alone fails to produce any detectable strand displacement product of 80 nt, which would correspond to the complete displacement of the RNA (Fig. 6), the formation of 70-nt circles must be the result of very limited extension by pol coupled with the nick translation activity of Fen-1 (1).

We confirmed the nick translation activity of Fen-1 on this RNA-containing P/T in the presence of wild-type or exo$^-$ HSV-1 pol (Fig. 7). The primer was labeled at the 5′ end, and unlabeled dNTPs were used for extension to permit accurate quantification (Table 1). As observed with the DNA P/Ts, Fen-1 alone produced predominantly 1- and 3-nt products with the RNA-containing P/T (Fig. 7A). However, the 3-nt product was observed in greater abundance than the 1-nt product following incubation with Fen-1. In addition, Fen-1 incubation

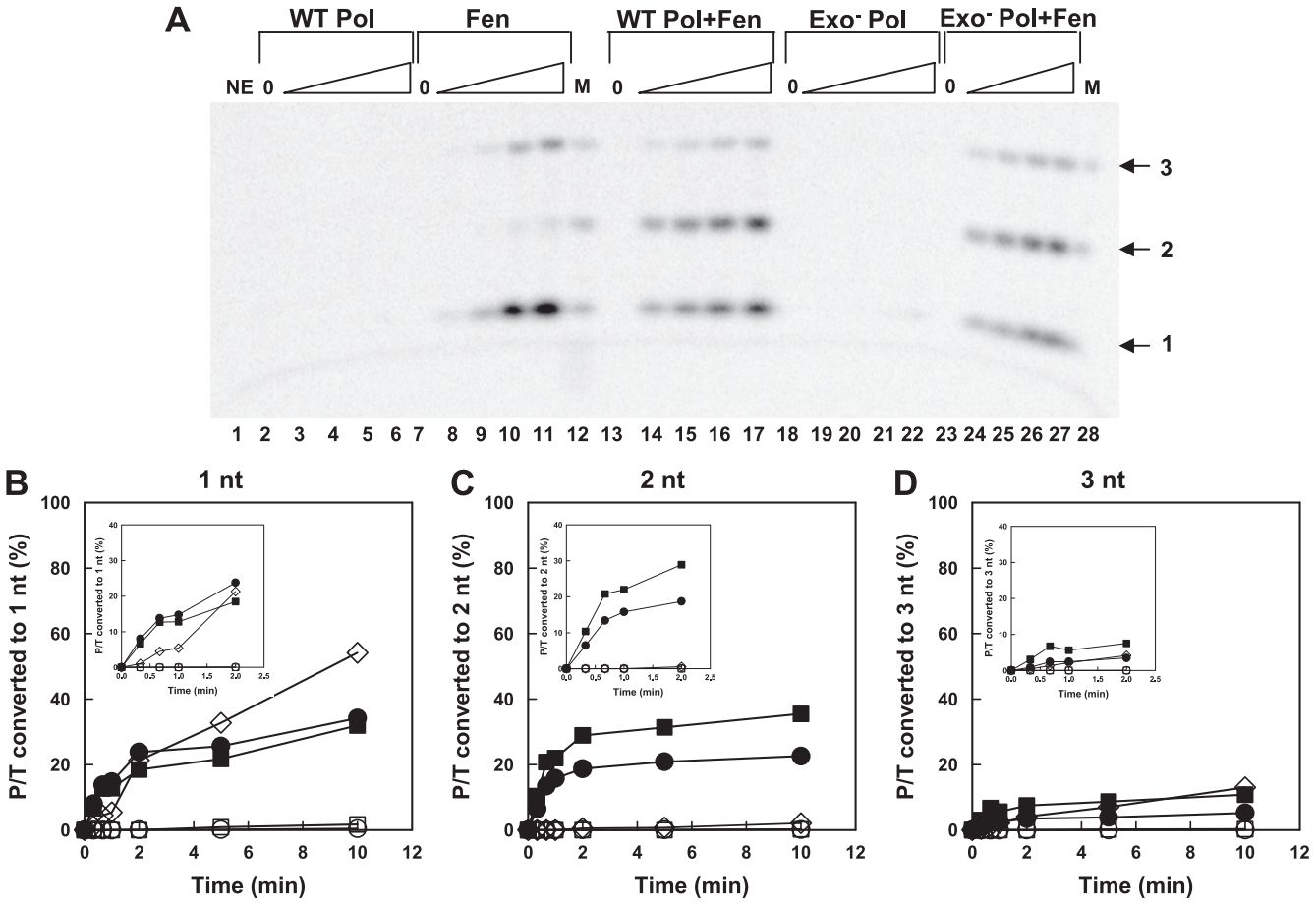

FIG. 5. Stimulation of human Fen-1 nick translation activity on DNA-containing primer/templates by HSV DNA polymerase. The 50/70 DNA-containing P/T was 5′ end labeled and used at a final concentration of 0.5 nM. (A) The P/T was incubated in the absence of enzyme (NE) but in the presence of EDTA (lane 1) or in the presence of 50 nM wild-type polymerase (WT Pol; lanes 2 to 6), Fen-1 (Fen) at a concentration of 0.01 U/μl (lanes 7 to 11), both enzymes together (WT Pol+Fen; lanes 13 to 17), 50 nM exo-deficient polymerase (Exo$^-$ Pol; lanes 18 to 22), or exo-deficient pol together with Fen-1 (Exo- Pol+Fen; lanes 23 to 27). Reactions marked 0 (lanes 2, 7, 13, 18, and 23) contained the indicated enzymes but were incubated for 10 min in the presence of EDTA. Otherwise, reactions were terminated by the addition of EDTA at increasing times up to 10 min. Products were separated by electrophoresis through long, sequencing-style denaturing gels containing 20% polyacrylamide and 7 M urea. In this gel, only four time points are shown for each enzyme combination, corresponding to 20 s (lanes 3, 8, 14, 19, and 24), 40 s (lanes 4, 9, 15, 20, and 25), 2 min (lanes 5, 10, 16, 21, and 26), and 5 min (lanes 6, 11, 17, 22, and 27). Only the portion of the gel containing the mono- (1), di- (2), and trinucleotides (3) (arrows) is shown. The marker (M) (lanes 12 and 28) was produced by the partial digestion of the labeled single-stranded 50-nt DNA primer strand with 3′-to-5′ exo activity of HSV-1 pol in the absence of added nucleotides. (B, C, and D) The radioactivity of each of the small products (1, 2, and 3 nt, respectively) during the entire reaction period was calculated as a percentage of total radioactivity loaded onto each lane and plotted as a function of time (○, wild-type pol; □, exo-deficient pol; ◇, Fen-1; ●, wild-type pol + Fen-1; ■, exo-deficient pol + Fen-1). The insets show the accumulation of products during the first 2 min. The initial rate of accumulation of each small product was estimated during the first 40 s from these data by least-squares analysis and is displayed in Table 1.

with the RNA-containing P/T yielded a 2-nt minor product. As observed with the DNA P/T, the incubation of the RNA-containing P/T with either wild-type or exo$^-$ pol alone yielded little, if any, labeled (1- to 3-nt) small products (Fig. 7A). The amount of 1-, 2-, or 3-nt product formed following the incubation of R_{10}40/70 P/T with different enzyme combinations was quantified and plotted as a function of time through 10 min (Fig. 7B, C, and D, respectively). In the presence of Fen-1 and HSV-1 wild-type or exo$^-$ pol, we observed a decreased initial rate of formation of 3-nt RNA product compared to that following incubation with Fen-1 alone. However, the initial rate of formation of the 1-nt product was enhanced approximately 3-fold by wild-type pol and more than 4-fold by exo$^-$ pol (Table 1). Likewise, the initial rate of formation of 2-nt product by Fen-1 on the RNA-containing P/T was significantly enhanced by either wild-type or exo$^-$ HSV-1 pol. Taken together, these results demonstrated that the nick translation activity of Fen-1 was enhanced by either the wild-type or exo$^-$ pol on RNA-containing substrates, and they confirm that the activities of the HSV-1 pol and Fen-1 act coordinately to produce small products, at least *in vitro*. Thus, these results account for the ability of the non-strand-displacing wild-type HSV-1 pol to produce ligatable product with RNA-containing P/Ts only in the presence of Fen-1 (Fig. 6, lanes 14 and 15).

Localization of Fen-1 in HSV-1-infected cells. To gain evidence that Fen-1 and HSV-1 pol proteins can work together *in vivo*, we examined their abilities to colocalize in viral DNA replication compartments in HSV-1-infected cells. To better

TABLE 1. Initial rates of removal of nucleotides from DNA- and RNA-containing primer/templates by Fen-1 and HSV-1 DNA polymerase

Enzyme(s)[a]	Initial rate of release (pM/min)[b]					
	50/70 DNA primer/template			R_{10}40/70 RNA-DNA		
	1 nt[a]	2 nt	3 nt	1 nt[a]	2 nt	3 nt
WT pol	0.21 ± 0.03	0.09 ± 0.02	0.03 ± 0.003	0.11 ± 0.01	0.07 ± 0.007	0.02 ± 0.006
WT pol + Fen-1	103 ± 11	100 ± 1.3	18.0 ± 2.6	107 ± 8.9	35.4 ± 5.7	36.5 ± 6.0
Fen-1	29.5 ± 5.0	1.1 ± 0.09	10.1 ± 2.1	36.5 ± 7.4	18.7 ± 3.3	82.8 ± 10
exo$^-$ pol	0.92 ± 0.07	0.10 ± 0.02	0.16 ± 0.02	1.1 ± 0.07	0.43 ± 0.03	ND[c]
exo$^-$ pol + Fen-1	94.8 ± 3.3	155 ± 1.3	50.0 ± 2.0	152 ± 7.5	160 ± 2.4	29.4 ± 0.6

[a] Reaction mixes contained 0.5 nM the indicated primer/template mixed with Fen-1 (0.01 U/μl) and/or 50 nM the catalytic subunits of the wild-type HSV-1 DNA polymerase (WT Pol) or exonuclease-deficient polymerase (exo$^-$ pol) as indicated.
[b] Rates (± standard deviations) were estimated by linear regression during the first 40 s of the reactions (Fig. 5 and 7) and were initiated by the addition of $MgCl_2$.
[c] ND, none detected.

visualize the localization of Fen-1, we transiently expressed a GFP-Fen-1 fusion protein in BHK cells, which are permissive for HSV-1 replication. It has been shown previously that GFP-Fen-1 associates with actively replicating DNA and concentrates in speckles known as replication foci (7, 46). Moreover, the localization of the transiently expressed GFP-Fen-1 is the same as that in stably transfected cell lines (46). BHK cells transfected with a plasmid encoding GFP-mouse Fen-1 were treated with BrdU for 30 min prior to fixation (48 h after transfection) and permeabilization to identify areas of active DNA synthesis. BrdU localization was detected by indirect immunofluorescence using BrdU monoclonal antibody as the primary antibody and RITC-conjugated goat anti-mouse IgG as the secondary antibody. Confocal microscopy was used to visualize the cells and to discriminate between the GFP (green) and RITC (red) localization patterns as described in Materials and Methods (Fig. 8A). GFP-Fen-1 has both a diffuse localization pattern within the nucleoplasm and a speckled pattern of more concentrated localization within nuclei (Fig. 8A, left), consistently with previous observations of GFP-Fen-1 localization (46). Actively replicating DNA is shown by the BrdU localization pattern in the middle panel. When both emission frequencies were observed together (Fig. 8A, right), the colocalization of GFP-Fen-1 within areas of active DNA replication could be readily detected (Fig. 8A). A Z-stack series was obtained to produce a three-dimensional projection of the colocalization of GFP-Fen-1 with active DNA replication sites in uninfected cells (Movie S1A [http://streaming.osu.edu/mediawww2/parris/FigS1A/]).

HSV-1 DNA replication takes place in globule-like areas, known as replication compartments, within infected cell nuclei, and the essential HSV-1-encoded DNA replication proteins, including ICP-8, the pol catalytic subunit, and the UL42 pol accessory protein, all colocalize within these compartments during productive virus replication (12, 18, 33, 35, 36, 43). We performed experiments similar to those outlined above to confirm that these replication compartments, as represented by the localization pattern of the HSV-1 UL42 pol accessory protein, coincide with regions of active DNA synthesis within BHK cells infected with HSV-1. BrdU was added to cells 30 min prior to fixation at 3 h postinfection. Permeabilized cells were analyzed by indirect immunofluorescence using mouse

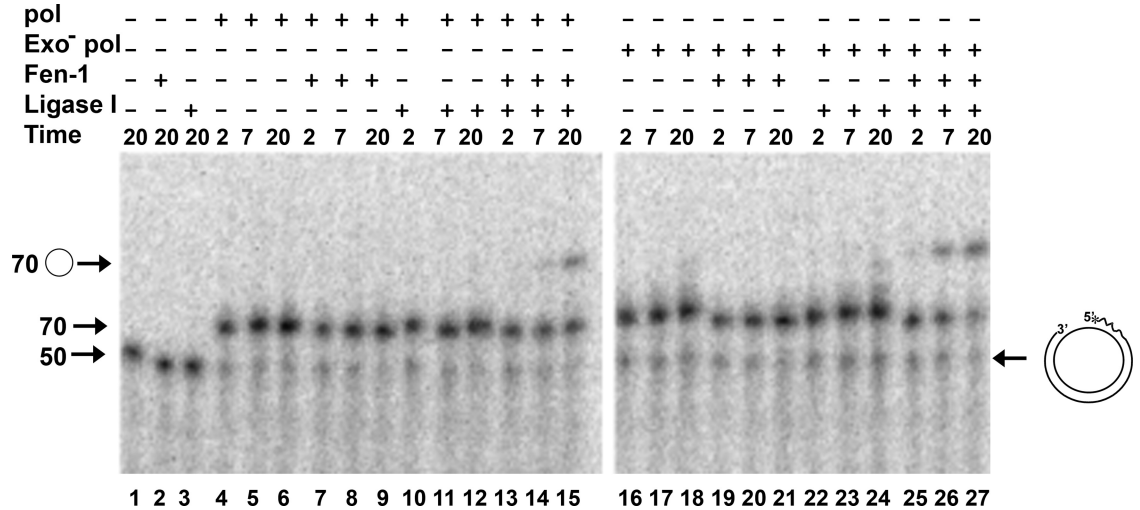

FIG. 6. Processing of RNA-containing primer/templates by HSV-1 polymerase, Fen-1, and DNA ligase I. The R_{10}40/70 P/T (Fig. 1E and depicted at the right in this figure) was used in all reactions and contained a 5′ end label on the primer. Reaction mixes included [α-^{32}P]dATP to track all products. The migration positions of 50- and 70-nt linear DNA oligonucleotides and 70-nt circular molecules are shown with arrows. The presence (+) or absence (−) of the indicated enzymes is shown. Reactions were performed as indicated in the legend to Fig. 4 and separated by electrophoresis through 10% denaturing polyacrylamide gels. Product formation was estimated as described in the text.

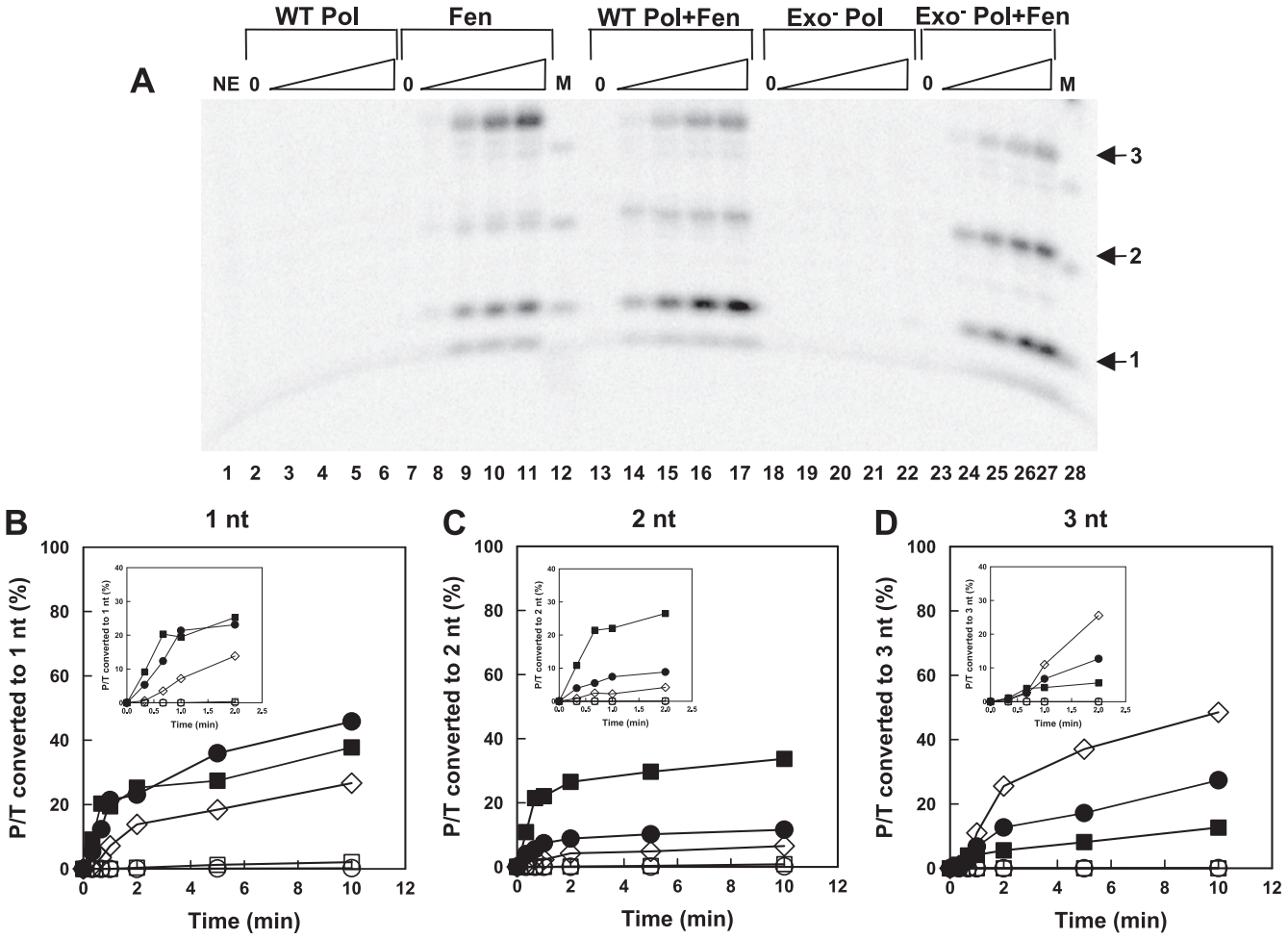

FIG. 7. RNA-containing P/T was incubated with wild-type or exo$^-$ HSV-1 DNA polymerase and/or human Fen-1 as indicated. Reactions were performed as described in the legend to Fig. 5 and did not include any radioactively labeled dNTP, thus permitting the accurate quantification of all products. (A) Products were separated by electrophoresis through long, sequencing-style denaturing gels containing 20% polyacrylamide and 7 M urea together with DNA markers (lanes 12 and 28) prepared as described in the legend to Fig. 5. RNA oligonucleotides migrate slightly slower than DNA oligonucleotides, and the positions of these are shown by the arrows on the right. In this gel, only four time points are shown for each enzyme combination, corresponding to 20 s (lanes 3, 8, 14, 19, and 24), 40 s (lanes 4, 9, 15, 20, and 25), 2 min (lanes 5, 10, 16, 21, and 26), and 5 min (lanes 6, 11, 17, 22, and 27). Reactions marked 0 (lanes 2, 7, 13, 18, and 23) contained the indicated enzymes but were incubated for 10 min in the presence of EDTA. (B, C, and D) The radioactivity of each of the small products (1, 2, and 3 nt, respectively) during the entire reaction period was calculated as a percentage of total radioactivity loaded onto each lane and plotted as a function of time (○, wild-type pol; □, exo-deficient pol; ◇, Fen-1; ●, wild-type pol + Fen-1; ■, exo-deficient pol + Fen-1). The insets show the accumulation of products during the first 2 min. The initial rate of accumulation of each small product was estimated during the first 40 s from these data by least-squares analysis and is displayed in Table 1.

monoclonal BrdU antibody and FITC-conjugated goat anti-mouse IgG to detect BrdU, as well as rabbit polyclonal antibody to the UL42-immundominant epitope and RITC-conjugated goat anti-rabbit IgG to detect UL42 (Fig. 8B). The typical globular-like replication compartments in which UL42 protein localizes are clearly visible at 3 h postinfection (Fig. 8B, middle). These structures are coincident with areas of active DNA replication, indicated by BrdU localization (Fig. 8B, left) and when the localization patterns of both proteins are visualized simultaneously (Fig. 8B, right). The pattern of BrdU localization in infected cells is clearly distinct from that in uninfected cells (compare Fig. 8A tozq Fig. 8B), suggesting that nearly all active DNA synthesis is viral. A three-dimensional projection of the colocalization of viral replication compartments (UL42, red) with sites of DNA synthesis (BrdU, green) is available in supplemental materials (Movie S1B [http://streaming.osu.edu/mediawww2/parris/FigS1B/]).

The ability of viral DNA replication to take place in discrete structures within the nuclei of infected cells provided an opportunity to determine whether or not Fen-1 could distribute to areas of active viral DNA synthesis. BHK cells were transfected with GFP-Fen-1 plasmid and then infected with HSV-1 42 h later at a multiplicity of infection (5 PFU/cell) sufficient to ensure that every cell in the population was infected. The localization of the UL42 polymerase accessory protein at 3 h postinfection was detected by indirect immunofluorescence with UL42 primary antibody and RITC-conjugated secondary antibody (Fig. 8C). Although GFP-Fen-1 could be found

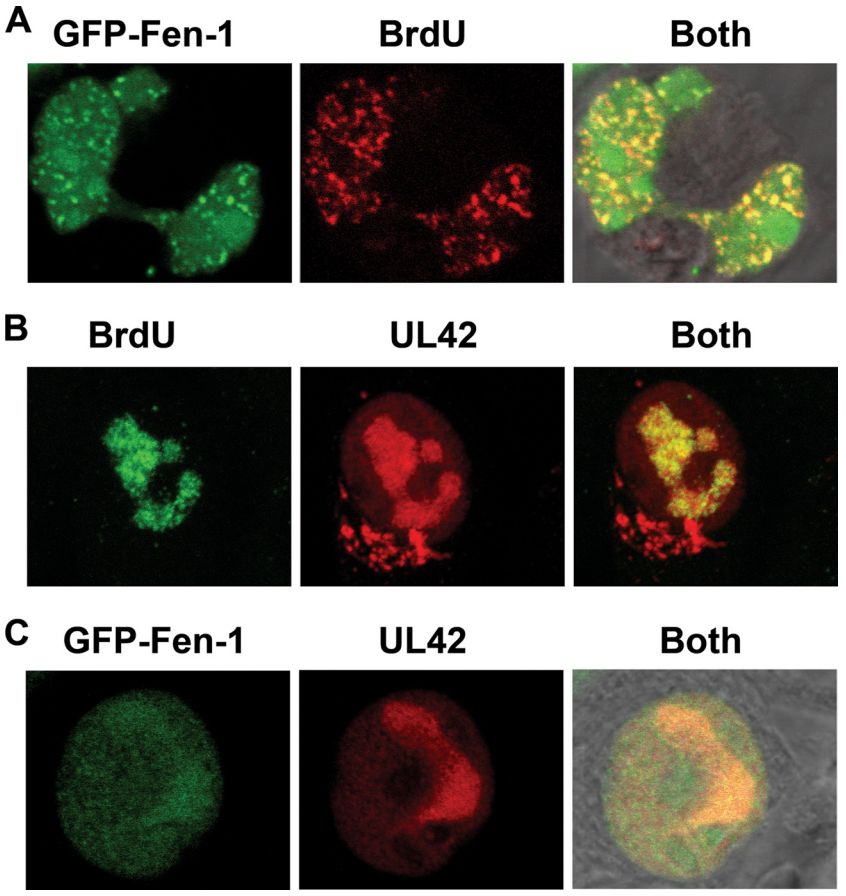

FIG. 8. Localization of Fen-1 and HSV-1 UL42 protein with replicating DNA in uninfected and infected cells. (A) BHK cells were transfected with 600 ng of plasmid expressing GFP-tagged Fen-1 (GFP-Fen-1). Thirty minutes prior to fixation (48 h posttransfection), BrdU was added to a final concentration of 100 μM to tag replicating DNA. Following fixation, cells were permeabilized with 0.25% Triton X-100 and incubated first with mouse monoclonal antibody to BrdU, followed by incubation with RITC-conjugated goat-anti-mouse antibody. Cells were viewed using a confocal microscope set to detect GFP-Fen-1 only as green color (left), BrdU only as red color (center), and the simultaneous localization of both (right). A multitrack mode was used to collect images sequentially. To ensure that there was no overlap in emission between channels, the green or red lasers were turned off sequentially prior to final image collection (data not shown). (B) BHK cells were infected with HSV-1 strain KOS at an input multiplicity of 5 PFU/cell and fixed at 3 h postinfection. Thirty minutes prior to fixation, BrdU was added to cultures. Cells were stained sequentially with BrdU mouse monoclonal antibody, FITC-conjugated goat anti-mouse IgG, primary polyclonal anti-peptide antibody UL42, the viral polymerase processivity factor, and secondary antibody RITC-conjugated goat anti-rabbit IgG. Images were collected as described in the text to detect the localization of BdrU in replicating DNA only (left) or HSV-1 UL42 only in infected cells (center). The colocalization of actively replicating DNA and viral replication compartments is shown by the yellow color (right). (C) BHK cells were transfected with plasmid (600 ng) expressing GFP-Fen-1 and infected 48 h later with HSV-1 (5 PFU/cell). Cells were fixed at 3 h postinfection, as indicated, and stained with rabbit antibody to UL42 and RITC-conjugated goat anti-rabbit IgG. Images were collected in multitrack mode to detect the localization of GFP-Fen-1 (left), UL42 (center), or both (right). A series of 20 Z-sections (0.35 μm thick) was obtained and used to create three-dimensional projections of the cells shown (Movie S1A to C).

localized throughout the nucleus in infected cells, it clearly concentrated within UL42-containing viral replication compartments (Fig. 8C, left and right). A three-dimensional projection of the colocalization of GFP-Fen-1 within replication compartments containing UL42 is available as supplemental material (Movie S1C [http://streaming.osu.edu/mediawww2/parris/FigS1C/]). Similar results demonstrating the colocalization of HSV-1 UL42 protein and GFP-Fen-1 were observed at many different multiplicities of infection and at times up to 6 h postinfection whenever both proteins were detected in the same cell (Y. Zhu and D. S. Parris, results not shown). Taken together, these results demonstrate that GFP-Fen-1 localizes within infected cells in a pattern distinct from that in uninfected cells, and it concentrates within the same areas that are associated with viral DNA replication.

Coimmunoprecipitation of host and viral DNA replication proteins. We investigated the ability of endogenous Fen-1 to associate with virus-encoded DNA replication proteins by coimmunoprecipitation analysis. Extracts of mock-infected or HSV-1-infected Vero cells were prepared and immunoprecipitated with mouse monoclonal antibody directed to human Fen-1, HSV-1 UL42 pol accessory protein, or an isotype control monoclonal antibody to human c-myc. Immunoprecipitated proteins then were separated by SDS-PAGE and identified by immunoblotting with various rabbit polyclonal antibodies to HSV-1 UL42, human PCNA, and human Fen-1.

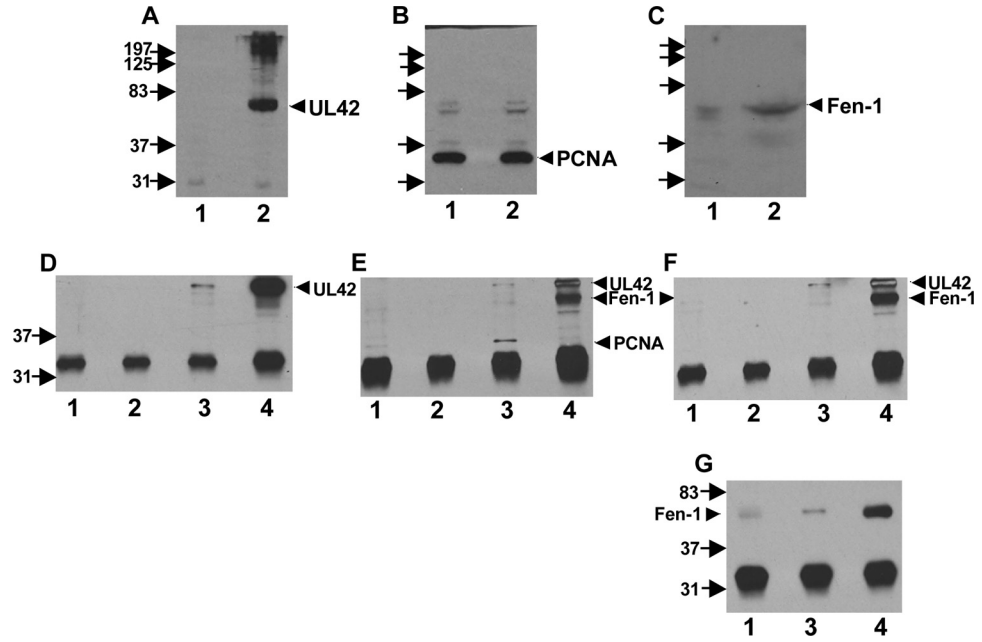

FIG. 9. Coimmunoprecipitation of Fen-1 with HSV-1 UL42. (A to C) Extracts of Vero cells that were mock infected (lane 1) or infected with HSV-1 at a multiplicity of infection of 10 PFU/cell and harvested at 8 h postinfection (lane 2) were prepared as described in Materials and Methods. The presence of UL42 (A), PCNA (B), and Fen-1 (C) in 10 μl extract (140 μg protein) was determined by immunoblotting using rabbit polyclonal anti-peptide antibody 834 directed to UL42 residues 360 to 377 (40), rabbit polyclonal antibody directed to a PCNA epitope mapping between residues 75 and 125, or rabbit polyclonal antibody directed to full-length human Fen-1. Primary antibodies were detected with horseradish peroxidase-conjugated goat-anti-rabbit IgG as described in Materials and Methods. The migration of molecular size standards (in kDa) is shown to the left. (D to G) Extracts from mock-infected (lane 1) or infected (lanes 2 to 4) cells were immunoprecipitated with monoclonal antibody to human Fen-1 (lanes 1 and 3), HSV-1 UL42 (lane 4), or the control human c-myc (lane 2). The immunoprecipitates were separated by SDS-PAGE and probed first for the presence of UL42 (D) and then stripped and probed successively with antibodies to Fen-1 (F) and PCNA (E) as described for panels A to C. In panel G, a portion of the immunoprecipitated material was separated on a distinct gel and probed with rabbit polyclonal antibody to Fen-1. There was an insufficient amount of the c-myc immunoprecipitate remaining for this purpose.

Figure 9A to C shows the relative amounts of the respective proteins present in the extracts of mock-infected versus infected cells and demonstrates the specificity of antibodies. As expected, no protein species reactive to HSV-1 UL42 antibody is present in mock-infected cells. Both PCNA and Fen-1 could be detected in mock-infected and infected cells, although there is more Fen-1 present in the infected than mock-infected cell extracts that were immunoprecipitated. Mock-infected and infected cell extracts were immunoprecipitated with Fen-1 antibody (Fig. 9 D to G, lanes 1 and 3, respectively), and immunoblots of separated proteins were probed for the presence of UL42 (Fig. 9D). In infected cells, a small amount of UL42 was present in Fen-1 immunoprecipitates but not in control c-myc-immunoprecipitates (Fig. 9D, lane 2). However, Fen-1 did not quantitatively immunoprecipitate UL42 from infected cells, as considerably more UL42 was immunoprecipitated by UL42-specific monoclonal antibody (Fig. 9D, lane 4). Blots were stripped and reprobed first with rabbit polyclonal antibody to Fen-1 (Fig. 9F), stripped again, and then probed with antibody to PCNA. PCNA was observed to coimmunoprecipitate with Fen-1 in both mock-infected (lane 1) and infected (lane 3) cells. The presence of PCNA in immunoprecipitates was deemed specific to interactions with Fen-1, since no PCNA was immunoprecipitated with the control c-myc antibody (Fig. 9E, lane 2) and is consistent with the known ability of Fen-1 to bind to PCNA (32). The low level of PCNA in anti-Fen-1 immunoprecipitates most likely reflects the low avidity of the antibody for its cognate protein and/or the transient nature of the association of Fen-1 with PCNA previously observed (46). Infected cells immunoprecipitated with monospecific antibody to UL42 pulled down not only UL42 (Fig. 9D, lane 4) but also Fen-1 (Fig. 9F, lane 4) and a small amount of PCNA (Fig. 9E, lane 4). Because the migration of Fen-1 is similar to that of a proteolytic fragment of UL42 present in the extracts and since the stripping of the UL42 signal was not complete, we separated another portion of immunoprecipitate and probed the blot with Fen-1 antibodies only (Fig. 9G). The results confirm that abundant Fen-1 was coimmunoprecipitated with UL42 antibody. The larger amount of Fen-1 that precipitated with UL42 antibody compared to that precipitated by cognate antibody might reflect the apparently larger quantity of Fen-1 present in the infected cell extracts, a higher efficiency of the immunoprecipitation of cognate (and associated proteins) with the UL42 antibody, or both.

DISCUSSION

Of the seven HSV-1 genes that are necessary and sufficient for origin-dependent DNA replication within cells, six of these (all except the origin binding protein) can initiate replication from ssDNA circles to form long concatemers of predominantly ssDNA (15, 26). In one study, synthesis from the com-

plementary template also was observed, although it was less efficient than synthesis from the leading-strand template and required a substantial delay (15). Products complementary to the lagging-strand template also were longer than expected for Okazaki fragments produced in mammalian cells. Such products are more consistent with the *de novo* initiation of the synthesis of products from the long single-stranded species rather than coordinated leading- and lagging-strand synthesis. These factors prompted us to search for cellular proteins that are likely to be involved in HSV lagging-strand synthesis and maturation. The results reported herein demonstrate the ability of a cellular protein, Fen-1, to cooperate with HSV-1 pol to obtain a ligatable product predicted to be an essential intermediate in the proper processing of lagging-strand intermediates. We present evidence that at least one activity of Fen-1 is stimulated by HSV-1 pol *in vitro*. That Fen-1 is involved in the replication of HSV DNA within mammalian cells is suggested by the fact that overexpressed GFP-Fen-1 accumulates within viral DNA replication compartments, and at least some of the endogenous Fen-1 within infected cells can be immunoprecipitated with the HSV-1 pol accessory protein.

Possible role of host Fen-1 in HSV-1 lagging-strand synthesis. To understand the events that must occur during the maturation of HSV-1 lagging-strand intermediates, it is important to understand how viral pol responds when encountering the 5′ end of a downstream Okazaki fragment. In *S. cerevisiae*, pol δ mutations in conserved sites I and II of the 3′-to-5′ exo domain were synthetically lethal with even mild Fen-1 mutations, suggesting that the 3′-to-5′ exo activity of pol δ was partially redundant with the activity of Fen-1 (23). Subsequent studies by the same group demonstrated that an important function of the exo activity of the wild-type pol δ was its ability to promote idling turnover to maintain a ligatable nick (17, 22). Indeed, *S. cerevisiae* exo$^-$ pol δ promoted strand displacement of ~5 nt upon encounter with a downstream 5′ end, and DNA ligase I failed to seal the products (22). We previously demonstrated that wild-type HSV-1 pol possesses strong idling-turnover activity with little or no strand displacement activity (62). Thus, the gap filling of a 50/70 DNA P/T by wild-type HSV-1 pol yielded a high proportion of products that could be sealed with DNA ligase I (Fig. 2). The strong idling-turnover activity of wild-type HSV-1 pol also allowed for the strand displacement of only 1 or 2 nt on a similar P/T, except that the primer contained 10 RNA residues at the 5′ end (Fig. 6). Nevertheless, the nick translation activity of Fen-1 was able to efficiently cleave these displaced residues, as they were formed by wild-type viral pol to produce circles that could be ligated with DNA ligase I. As expected if the Fen-1 and viral pol activities were coordinated, increased strand displacement activity through the RNA primer by exo$^-$ pol compared to that of wild-type pol increased the rate of the appearance of ligated product (Fig. 6, compare lanes 25 to 27 to lanes 13 to 15). It is interesting that the wild-type and exo$^-$ HSV-1 pol catalytic subunits promoted the formation of the 1-nt products of the nick translation activity of Fen-1 to similar degrees on either annealed DNA- or RNA-containing P/Ts (Fig. 5 and 7 and Table 1). This is in contrast to the preferential ability of pol δ to stimulate the nick translation activity of Fen-1 on RNA/DNA compared to that on DNA/DNA hybrids (48). We were unable to perform similar nick translation experiments with the processive HSV-1 pol/UL42 because of its failure to dissociate from P/Ts under these reaction conditions, thus limiting the access of Fen-1 and DNA ligase I to the P/T (Zhu and Parris, unpublished). However, we confirmed that the products of gap-filling synthesis by pol/UL42 on flapped and unflapped P/Ts were indistinguishable from those of the pol catalytic subunit (62 and results not shown). Taken together, these results demonstrate the inherent ability of the HSV-1 pol catalytic subunit to coordinate its activity with that of human Fen-1 to yield the ligatable products required for correct and efficient Okazaki fragment maturation.

Fen-1 colocalizes with essential viral DNA replication proteins in HSV-1-infected cells. If Fen-1 is involved in the processing of HSV-1 lagging-strand intermediates *in vivo*, it must be present at the site(s) of viral DNA replication. It was previously demonstrated that ectopically expressed fluorescent protein fusions of Fen-1 and PCNA colocalized with BrdU within DNA replication foci of cells (46). We confirmed this localization by the confocal microscopy of transiently expressed GFP-Fen I in uninfected BHK cells (Fig. 8A). The GFP-Fen-1 localization pattern changed dramatically by 3 h after the infection of cells with HSV-1 (compare Fig. 8A and C), with most areas of major accumulation coincident with those in which the highest concentrations of UL42 (and replicating viral DNA) are found (Fig. 8C; also see Movie S1C). The ability of overexpressed Fen-1 to accumulate within replication compartments in HSV-1-infected cells provides strong evidence in support of a role for Fen-1 in viral DNA synthesis. The association of Fen-1 with replication compartments appears to be specific, since endogenous Fen-1 immunoprecipitates with the HSV-1 pol accessory protein UL42 in infected cells. Whether or not Fen-1 interacts directly with UL42 could not be determined in these experiments, as UL42 forms a stable heterodimer with pol (29) and also can functionally interact with the HSV-1 origin binding protein, UL9 (55). Because of the high background and low avidity of available antibodies to HSV-1 pol, we were unable to determine whether or not Fen-1 and pol could be coimmunoprecipitated. The small amount of PCNA that coimmunoprecipitated with UL42 in infected cells could reflect interactions of PCNA with Fen-1, UL42, and/or other proteins that interact directly or indirectly with UL42. More work will be necessary to investigate the ability of Fen-1 to interact with individual viral replication proteins and to determine the stoichiometry of these interactions.

Although Fen-1 in conjunction with HSV-1 pol can produce structures that can be ligated with DNA ligase I, evidence still is lacking for a specific role of DNA ligase I in HSV-1 DNA synthesis. Indeed, DNA ligase I is not absolutely essential for HSV-1 DNA replication, since HSV-1 has been shown to replicate in cells in which DNA ligase I activity is knocked down (42). It should be pointed out that although DNA ligase I is considered to be the major ligase involved in DNA replication in mammalian cells, it is not absolutely essential, presumably because other ligases can compensate for the absence of DNA ligase I to fulfill replication activity, though with reduced efficiency (3). Thus, it is possible that a ligase other than or in addition to DNA ligase I functions to seal viral lagging-strand intermediates.

So how might Fen-1 function during the replication of HSV

DNA? Our *in vitro* results demonstrate that the nick translation activity of Fen-1 is promoted by the wild-type viral pol catalytic subunit despite the poor strand displacement activity of pol. Moreover, strand displacement by wild-type pol is promoted by the successive cleavage of small flaps by Fen-1 to generate ligatable nicks. Based on this apparent coordination of activities, it is intriguing to speculate that Fen-1 operates close to the replication fork to assist the viral polymerase in the processing of lagging-strand intermediates. However, it remains possible that the accumulation of Fen-1 within replication compartments in HSV-1-infected cells reflects an entirely different role. Indeed, a variety of proteins associated with DNA repair have been found to colocalize within replication compartments (60) or to be associated with essential HSV DNA replication proteins (49), though the specific roles that these proteins play in viral DNA replication have yet to be determined.

Our findings that Fen-1 appears to be redirected from the regions of cellular DNA synthesis to distinct sites for viral DNA replication pose another important question: how is it directed to viral replication compartments? One possibility is through direct interaction with the viral pol catalytic subunit. This is an attractive hypothesis due to the ability of HSV-1 pol to coordinate closely with Fen-1 to process lagging-strand intermediates *in vitro*. While such coordination could be facilitated by direct physical interactions, to date no direct physical interactions between Fen-1 and HSV-1 pol have been reported. Nevertheless, the ability of both UL42 and Fen-1 antibodies to coimmunoprecipitate the respective noncognate protein suggests a tight interaction with one or more constituent proteins of the HSV-1 DNA replication complex. A second possibility for redirecting Fen-1 to sites of viral DNA replication *in vivo* is PCNA. Fen-1 localizes to sites of cellular DNA replication through its physical and functional interactions with PCNA (31, 32, 53). However, the high mobility of Fen-1 and DNA ligase I compared to that of PCNA (46, 47) suggests that PCNA serves as a stable platform onto which Fen-1 and DNA ligase I are loaded for the efficient processing of cellular lagging-strand intermediates. The mobile nature of Fen-1 also would permit its rapid relocalization to sites of viral DNA synthesis if PCNA (or other proteins with which it interacts) also were attracted to those sites. In fact, PCNA has been shown to localize within HSV DNA replication compartments (59 and Zhu and Parris, unpublished) and could be coimmunoprecipitated with the ssDNA binding protein, ICP-8 (49), a protein that is essential for the formation of the globule-like replication compartments (12, 18, 35). These results are consistent with those of the current study that demonstrate PCNA in immunoprecipitates with UL42 antibody. Thus, we propose a model in which one or more HSV-1 DNA replication proteins, such as ICP-8 or UL42, attracts PCNA, together with the PCNA-interacting proteins, Fen-1 and DNA ligase I, to sites of viral DNA synthesis, where these cellular proteins can function with the viral polymerase (and other essential viral DNA replication proteins) in the synthesis and maturation of lagging-strand intermediates. The increasing number of possible cellular proteins involved in this process will present continued challenges to developing a fully *in vitro* system that recapitulates efficient leading- as well as lagging-strand synthesis.

ACKNOWLEDGMENTS

This work was supported in part by the National Institutes of Health (GM 073832 to D.S.P. and CA 09338 training grant to Y.Z.), the American Cancer Society Ohio Division (to D.S.P.), and by grants from the German Research Council DFG (to M.C.C.).

Core services (D.S.P.) were provided by the Department of Molecular Virology, Immunology, and Medical Genetics, College of Medicine, and Comprehensive Cancer Center at the Ohio State University.

REFERENCES

1. **Ayyagari, R., X. V. Gomes, D. A. Gordenin, and P. M. J. Burgers.** 2003. Okazaki fragment maturation in yeast. I. Distribution of functions between Fen1 and Dna2. J. Biol. Chem. **278:**1618–1625.
2. **Bae, S.-H., and Y.-S. Seo.** 2000. Characterization of the enzymatic properties of the yeast Dna2 helicase/endonuclease suggests a new model for Okazaki fragment processing. J. Biol. Chem. **275:**38022–38031.
3. **Bentley, D. J., C. Harrison, A.-M. Ketchen, N. J. Redhead, K. Samuel, M. Waterfall, J. D. Ansell, and D. W. Melton.** 2002. DNA ligase I null mouse cells show normal DNA repair activity but altered DNA replication and reduced genome stability. J. Cell Sci. **115:**1551–1561.
4. **Biswal, N., B. K. Murry, and M. Benyish-Melnick.** 1974. Ribonucleotides in newly synthesized DNA of herpes simplex virus. Virology **69:**87–99.
5. **Boehmer, P. E., and A. V. Nimonkar.** 2003. Herpes virus replication. IUBMB Life **55:**13–22.
6. **Burgers, P. M.** 2009. Polymerase dynamics at the eukaryotic DNA replication fork. J. Biol. Chem. **284:**4041–4045.
7. **Cardoso, M. C., C. Joseph, H. P. Rahn, R. Reusch, B. Nadal-Ginard, and H. Leonhardt.** 1997. Mapping and use of a sequence that targets DNA ligase I to sites of DNA replication in vivo. J. Cell Biol. **139:**579–587.
8. **Chaudhuri, M., and D. S. Parris.** 2002. Evidence against a simple tethering model for enhancement of herpes simplex virus DNA polymerase processivity by accessory protein UL42. J. Virol. **76:**10270–10281.
9. **Chaudhuri, M., L. Song, and D. S. Parris.** 2003. The herpes simplex virus type 1 DNA polymerase processivity factor increases fidelity without altering pre-steady-state rate constants for polymerization or excision. J. Biol. Chem. **278:**8996–9004.
10. **Costa, R. H., K. G. Draper, L. Banks, K. L. Powell, G. Cohen, R. Eisenberg, and E. K. Wagner.** 1983. High-resolution characterization of herpes simplex virus type 1 transcripts encoding alkaline exonuclease and a 50,000-dalton protein tentatively identified as a capsid protein. J. Virol. **48:**591–603.
11. **Crute, J. J., and I. R. Lehman.** 1991. Herpes simplex virus-1 helicase-primase. J. Biol. Chem. **266:**4484–4488.
12. **de Bruyn Kops, A., and D. M. Knipe.** 1988. Formation of DNA replication structures in herpes virus-infected cells requires a viral DNA binding protein. Cell **55:**857–868.
13. **Dodson, M. S., and I. R. Lehman.** 1991. Association of DNA helicase and primase activities with a subassembly of the herpes simplex virus 1 helicase-primase composed of the UL5 and UL52 gene products. Proc. Natl. Acad. Sci. U. S. A. **88:**1105–1109.
14. **Dracheva, S., E. V. Koonin, and J. J. Crute.** 1995. Identification of the primase active site of the herpes simplex virus type 1 helicase-primase. J. Biol. Chem. **270:**14148–14153.
15. **Falkenberg, M., I. R. Lehman, and P. Elias.** 2000. Leading and lagging strand DNA synthesis *in vitro* by a reconstituted herpes simplex virus type 1 replisome. Proc. Natl. Acad. Sci. U. S. A. **97:**3896–3900.
16. **Garg, P., and P. M. J. Burgers.** 2005. DNA polymerases that propagate the eukaryotic DNA replication fork. Crit. Rev. Biochem. Mol. Biol. **40:**115–128.
17. **Garg, P., C. M. Stith, N. Sabouri, E. Johansson, and P. M. Burgers.** 2004. Idling by DNA polymerase δ maintains a ligatable nick during lagging-strand DNA replication. Genes Dev. **18:**2764–2773.
18. **Goodrich, L. D., P. A. Schaffer, D. I. Dorsky, C. S. Crumpacker, and D. S. Parris.** 1990. Localization of the herpes simplex virus type 1 65-kilodalton DNA-binding protein and DNA polymerase in the presence and absence of viral DNA synthesis. J. Virol. **64:**5738–5749.
19. **Henricksen, L. A., J. Veeraraghavan, D. R. Chafin, and R. A. Bambara.** 2002. DNA ligase I competes with FEN1 to expand repetitive DNA sequences *in vitro*. J. Biol. Chem. **277:**22361–22369.
20. **Hoffmann, P. J., and Y. C. Cheng.** 1978. The deoxyribonuclease induced after infection of KB cells by herpes simplex virus type 1 or type 2. I. Purification and characterization of the enzyme. J. Biol. Chem. **253:**3557–3562.
21. **Jacob, R. J., and B. Roizman.** 1977. Anatomy of herpes simplex virus DNA. VIII. Properties of the replicating DNA. J. Virol. **23:**394–411.
22. **Jin, Y. H., R. Ayyagari, M. A. Resnick, D. A. Gordenin, and P. M. J. Burgers.** 2003. Okazaki fragment maturation in yeast. II. Cooperation between the polymerase and 3′-5′-exonuclease activities of pol δ in the creation of a ligatable nick. J. Biol. Chem. **278:**1626–1633.
23. **Jin, Y. H., R. Obert, P. M. J. Burgers, T. A. Kunkel, M. A. Resnick, and D. A. Gordenin.** 2001. The 3′ to 5′ exonuclease of DNA polymerase δ can substitute for the 5′ flap endonuclease Rad27/Fen1 in processing Okazaki frag-

ments and preventing genome instability. Proc. Natl. Acad. Sci. U. S. A. **98:**5122–5127.
24. **Johnson, R. E., G. K. Kovvali, L. Prakash, and S. Prakash.** 1998. Role of yeast Rth1 nuclease and its homologs in mutation avoidance, DNA repair, and DNA replication. Curr. Genet. **34:**21–29.
25. **Kao, H.-I., and R. A. Bambara.** 2003. The protein components and mechanism of eukaryotic Okazaki fragment maturation. Crit. Rev. Biochem. Mol. Biol. **38:**433–452.
26. **Klinedinst, D. K., and M. D. Challberg.** 1994. Helicase-primase complex of herpes simplex virus type 1: a mutation in the UL52 subunit abolishes primase activity. J. Virol. **68:**3693–3701.
27. **Knopf, K.-W.** 1979. Properties of herpes simplex virus DNA polymerase and characterization of its associated exonuclease activity. Eur. J. Biochem. **98:** 231–244.
28. **Kühn, F. J. P., and C. W. Knopf.** 1996. Herpes simplex virus type 1 DNA polymerase. Mutational analysis of the 3′-5′-exonuclease domain. J. Biol. Chem. **271:**29245–29254.
29. **Lehman, I. R., and P. E. Boehmer.** 1999. Replication of herpes simplex virus DNA. J. Biol. Chem. **274:**28059–28062.
30. **Levin, D. S., W. Bai, N. Yao, M. O'Donnell, and A. E. Tomkinson.** 1997. An interaction between DNA ligase I and proliferating cell nuclear antigen: implications for Okazaki fragment synthesis and joining. Proc. Natl. Acad. Sci. U. S. A. **94:**12863–12868.
31. **Levin, D. S., A. E. McKenna, T. A. Motycka, Y. Matsumoto, and A. E. Tomkinson.** 2000. Interaction between PCNA and DNA ligase I is critical for joining of Okazaki fragments and long-patch base-excision repair. Curr. Biol. **10:**919–922.
32. **Li, X., J. Li, J. Harrington, M. R. Lieber, and P. M. J. Burgers.** 1995. Lagging strand DNA synthesis at the eukaryotic replication fork involves binding and stimulation of FEN-1 by proliferating cell nuclear antigen. J. Biol. Chem. **270:**22109–22112.
33. **Liptak, L. M., S. L. Uprichard, and D. M. Knipe.** 1996. Functional order of assembly of herpes simplex virus DNA replication proteins into prereplicative site structures. J. Virol. **70:**1759–1767.
34. **Liu, Y., H.-I. Kao, and R. A. Bambara.** 2004. Flap endonuclease 1: a central component of DNA metabolism. Annu. Rev. Biochem. **73:**589–615.
35. **Lukonis, C. J., and S. K. Weller.** 1996. Characterization of nuclear structures in cells infected with herpes simplex virus type 1 in the absence of viral DNA replication. J. Virol. **70:**1751–1758.
36. **Lukonis, C. J., and S. K. Weller.** 1997. Formation of herpes simplex virus type 1 replication compartments by transfection: requirements and localization to nuclear domain 10. J. Virol. **71:**2390–2399.
37. **Maga, G., G. Villani, V. Tillement, M. Stucki, G. A. Locatelli, I. Frouin, S. Spadari, and U. Hübscher.** 2001. Okazaki fragment processing: modulation of the strand displacement activity of DNA polymerase δ by the concerted action of replicaiton protein A, proliferating cell nuclear antigen, and flap endonuclease-1. Proc. Natl. Acad. Sci. U. S. A. **98:**14298–14303.
38. **Marintcheva, B., and S. K. Weller.** 2001. A tale of two HSV-1 helicases: roles of phage and animal virus helicases in DNA replication and recombination. Prog. Nucleic Acid Res. Mol. Biol. **70:**77–118.
39. **Martin, I. V., and S. A. MacNeill.** 2002. ATP-dependent DNA ligases. Genome Biol. **3:**3005.1–3005.7.
40. **Monahan, S. J., T. F. Barlam, C. S. Crumpacker, and D. S. Parris.** 1993. Two regions of the herpes simplex virus type 1 UL42 protein are required for its functional interaction with the viral DNA polymerase. J. Virol. **67:**5922–5931.
41. **Murphy, M., P. Schenk, H. M. Linkinen, A. M. Cross, P. Taylor, A. Owsianka, R. G. Hope, H. Ludwig, and H. S. Marsden.** 1989. Mapping of epitopes of the 65K DNA-binding protein of herpes simplex virus type 1. J. Gen. Virol. **70:**2357–2364.
42. **Muylaert, I., and P. Elias.** 2007. Knockdown of DNA ligase IV/XRCC4 by RNA interference inhibits herpes simplex virus type 1 DNA replication. J. Biol. Chem. **282:**10865–10872.
43. **Olivo, P. D., J. J. Nelson, and M. D. Challberg.** 1989. Herpes simplex virus type 1 gene products required for DNA replication: identification and overexpression. J. Virol. **63:**196–204.
44. **Rossi, M. L., and R. A. Bambara.** 2006. Reconstituted Okazaki fragment processing indicates two pathways of primer removal. J. Biol. Chem. **281:** 26051–26061.
45. **Song, L., M. Chaudhuri, C. W. Knopf, and D. S. Parris.** 2004. Contribution of the 3′- to 5′-exonuclease activity of herpes simplex virus type 1 DNA polymerase to the fidelity of DNA synthesis. J. Biol. Chem. **279:**18535–18543.
46. **Sporbert, A., P. Domaing, H. Leonhardt, and M. C. Cardoso.** 2005. PCNA acts as a stationary loading platform for transiently interacting Okazaki fragment maturation proteins. Nucleic Acids Res. **33:**3521–3528.
47. **Sporbert, A., A. Gahl, R. Ankerhold, H. Leonhardt, and M. C. Cardoso.** 2002. DNA polymerase clamp shows little turnover at established replication sites but sequential de novo assembly at adjacent origin clusters. Mol. Cell **10:**1355–1365.
48. **Stith, C. M., J. Sterling, M. A. Resnick, D. A. Gordenin, and P. M. Burgers.** 2008. Flexibility of eukaryotic Okazaki fragment maturation through regulated strand displacement synthesis. J. Biol. Chem. **283:**34129–34140.
49. **Taylor, T. J., and D. M. Knipe.** 2004. Proteomics of herpes simplex virus replication compartments: association of cellular DNA replication, repair, recombination, and chromatin remodeling proteins with ICP8. J. Virol. **78:** 5856–5866.
50. **Timson, D. J., M. R. Singleton, and D. B. Wigley.** 2000. DNA ligases in the repair and replication of DNA. Mutat. Res. **460:**301–318.
51. **Tishkoff, D. X., A. L. Boerger, P. Bertrand, N. Filosi, G. M. Gaida, M. F. Kane, and R. D. Kolodner.** 1997. Identification and characterization of *Saccharomyces cerevisiae* EXO1, a gene encoding an exonuclease that interacts with MSH2. Proc. Natl. Acad. Sci. U. S. A. **94:**7487–7492.
52. **Tom, S., L. A. Henricksen, and R. A. Bambara.** 2000. Mechanism whereby proliferating cell nuclear antigen stimulates flap endonuclease 1. J. Biol. Chem. **275:**10498–10505.
53. **Tom, S., L. A. Henricksen, M. S. Park, and R. A. Bambara.** 2001. DNA ligase I and proliferating cell nuclear antigen form a functional complex. J. Biol. Chem. **276:**24817–24825.
54. **Tomkinson, A. E., N. J. Tappe, and E. C. Friedberg.** 1992. DNA ligase I from *Saccharomyces cerevisiae*: physical and biochemical characterization of the CDC9 gene product. Biochemistry **47:**11762–11771.
55. **Trego, K. S., and D. S. Parris.** 2003. Functional interaction between the HSV-1 polymerase processivity factor and origin-binding proteins: enhancement of UL9 helicase activity. J. Virol. **77:**12646–12659.
56. **Turchi, J. J., and R. A. Bambara.** 1993. Completion of mammalian lagging strand DNA replication using purified proteins. J. Biol. Chem. **268:**15136–15141.
57. **Waga, S., G. Bauer, and B. Stillman.** 1994. Reconstitution of complete SV40 DNA replication with purified replication factors. J. Biol. Chem. **269:**10923–10934.
58. **Waga, S., and B. Stillman.** 1998. The DNA replication fork in eukaryotic cells. Annu. Rev. Biochem. **67:**721–751.
59. **Wilcock, D., and D. P. Lane.** 1991. Localization of p53, retinoblastoma and host replication proteins at sites of viral replication in herpes-infected cells. Nature **349:**429–431.
60. **Wilkinson, D. E., and S. K. Weller.** 2004. Recruitment of cellular recombination and repair proteins to sites of herpes simplex virus type 1 DNA replication is dependent on the composition of viral proteins within prereplicative sites and correlates with the induction of the DNA damage response. J. Virol. **78:**4783–4796.
61. **Zheng, L., H. Dai, J. Qiu, Q. Huang, and B. Shen.** 2007. Disruption of the FEN-1/PCNA interaction results in DNA replication defects, pulmonary hypoplasia, pancytopenia, and newborn lethality in mice. Mol. Cell. Biol. **27:**3176–3186.
62. **Zhu, Y., K. S. Trego, L. Song, and D. S. Parris.** 2003. 3′ To 5′ exonuclease activity of herpes simplex virus type 1 DNA polymerase modulates its strand displacement activity. J. Virol. **77:**10147–10153.